Jurnal Riset Kimia

ISSN (print) : 1978-628X
ISSN (online) : 2476-8960

Profile of a Composite Based on Bacterial Cellulose and Polyvinyl Alcohol as a Drug Release Matrix for Tetracycline Hydrochloride

Afif Dwi Sukmaningrum[1], Emmy Yuanita[1], Ni Komang Tri Dharmayani[1], Sudirman[1], Ni Made Sudewianingsih[2], and Maria Ulfa[1]*

[1]Chemistry Department, Faculty of Mathematics and Natural Science, University of Mataram, Mataram-NTB, Indonesia

[2]Biology Laboratory, Faculty of Mathematics and Natural Science, University of Mataram, Mataram-NTB, Indonesia

Corresponding Author:
Maria Ulfa
ulfaarief@unram.ac.id

Received: February 2024
Accepted: September 2024
Published: September 2024

Abstract

Bacterial cellulose (BC) is a natural polymer with good mechanical properties and hydrophilicity. Polyvinyl alcohol (PVA) is a synthetic polymer widely used in medicine. Both have been researched for their potential in drug release and acceptance. This study aims to determine the role of BC and PVA as drug release matrices for tetracycline hydrochloride (TCH), with additional fillers such as graphite (G) and TiO_2. The results showed that the composites with BC matrix had lower mechanical properties than those with PVA matrix, with tensile strength values of 6.4075 and 17.446 MPa, respectively. However, the BC matrix was superior in porosity and swelling ability. The drug release testing of TCH from the composites showed that the appropriate model to describe drug release in BC matrix composites was in zero order, while the PVA matrix was in first order. The antibacterial activity of the composites on both matrices was tested against *Staphylococcus aureus*. The results indicate that both composites have potential applications in promising biomedical fields.

Keywords: *Bacterial cellulose; polyvinyl alcohol; graphite; TiO_2; tetracycline hydrochloride*.

Introduction

Controlling the release of drugs is a common practice, but designing drug release mechanisms is a complex process that requires extensive research. The drug release system aims to regulate the release of active ingredients from a drug by the desired purpose and importance of the drug[1]. Tetracycline hydrochloride (TCH) is an antibiotic commonly used to treat or prevent infections of the skin and bones caused by bacteria through enzymatic reactions, protein synthesis, and ribosomes. It can also modify the synthesis of the cytoplasmic membrane[2][3]. Controlling the drug release system of tetracycline hydrochloride is essential in accelerating the regeneration of osteoblasts, fibroblasts, and various cell types closely related to wound recovery, especially in the skin[2].

Bacterial cellulose (BC) has garnered attention in various fields due to its versatility as a biomaterial. It can be utilized in numerous ways, one of which is in the biomedical field. BC is beneficial in wound treatment, organ regeneration, disease diagnosis, and drug transportation[4].

Another popular polymer in biomedicine is polyvinyl alcohol (PVA). PVA is a synthetic

DOI: https://doi.org/ 10.25077/jrk.v15i2.692

polymer commonly used in this field due to its low protein absorption, biocompatibility, hydrophilicity, and high chemical resistance[5]. Research conducted by Leitão et al.[6] shows that PVA can have a more controlled impact on solution diffusion in composites.

Controlled release of TCH drug can be achieved by mixing it with two types of polymers, namely BC and PVA, to form a composite[7][8]. Composites combine two or more materials, producing heterogeneous reinforcement between the matrix and filler. In composites, the matrix is a place to distribute the filler load, usually in polymers, ceramics, and metals[9]. The filler in composites can be a particle or fiber that functions as a support and can come from nature or synthesis. Graphite (G) and titanium dioxide (TiO_2)[10][11] are some fillers that can support the performance of BC and PVA to be applied in the medical field with both antibacterial and mechanical activity. Graphite and its derivatives have been proven to resist bacteria and damage the bacterial cell membrane when subjected to graphite sheets[12]. Other chemical compounds, such as titanium dioxide (TiO_2), have antibacterial activity through the formation of reactive oxygen species (ROS) compounds, as demonstrated by research conducted by Pathakoti and colleagues[13].

In this study, two different methods were used to examine the drug release system of TCH on different composite matrices. The BC matrix composite was synthesized using immersion[10], while the casting method[14] was used for the PVA matrix composite. Different synthesis methods aimed to determine the drug release kinetics model of the two composite matrices. The research aimed to conduct a profile study of BC and PVA-based composites with G and TiO_2 fillers as a TCH drug release matrix.

Experimental

Materials

The materials used in this study were BC obtained from UMKM Yogyakarta, polyvinyl alcohol, graphite (Merck), potassium persulfate (Sigma-Aldrich), sodium hydroxide (Merck), n-butanol 80% (v/v) (Sigma-Aldrich), tetracycline hydrochloride (Merck), cetyl trimethyl ammonium bromide (Merck), buffer solution (Merck), methanol 96% (v/v) (Merck), and titanium dioxide (Merck).

Equipment/Instruments

The research was conducted using standard laboratory glassware, along with various equipment, including a hot plate stirrer (IKA C-MAG HS 7), FT-IR instrument (PerkinElmer), oven (Memmert), ultrasonication device (Trias Nathomi Chemindo), furnace (ThermoScientific), analytical balance (Fujitsu), pH meter (RoHS), EDS instrument (JEOL JCM-7000), digital screw micrometer (T&E CR1632), UV-Vis spectrophotometer instrument (Thermofisher), and tensilon (INSTRON 5567).

Methods

Purification of Bacterial Cellulose

BC was obtained from UMKM NATA Yogyakarta and produced using *Gluconacetobacter xylinus* bacteria with coconut water media. Bacterial cellulose was purified by washing and heating repeatedly (5 times), then soaked in 0.5 M NaOH (24 hours). Then BC was rewashed with water until pH = 7.

Fabrication of BC-Based Composite

According to Figure 1, to create the composite material start by calcining 5 g of graphite in a furnace at 1000 °C for 5 minutes. Then, homogenize the graphite (0.5% w/v) with CTAB (0.3% w/w) using ultrasonication for 7 hours[10]. Next, soak the BC in a graphite solution (0.5% w/v) and homogenize it using ultrasonication for 7 hours. After homogenization, bathe the BC/G composite in a mixture of PVA 3% (w/v), TiO_2 1% (w/v), and potassium persulfate 4% (w/v) and sonicate at 55 °C for 3 hours. Finally, dry the composite at room temperature for two days.

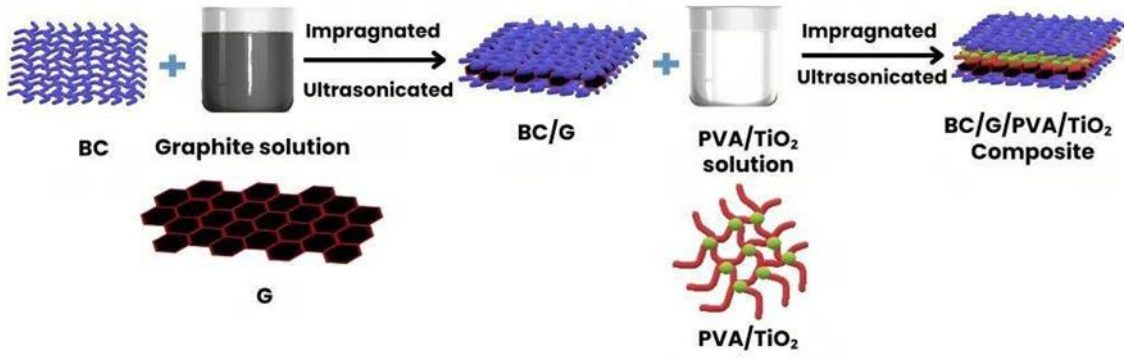

Figure 1. Schematic illustration of a method for synthesized BC/G/PVA/TiO_2 composite

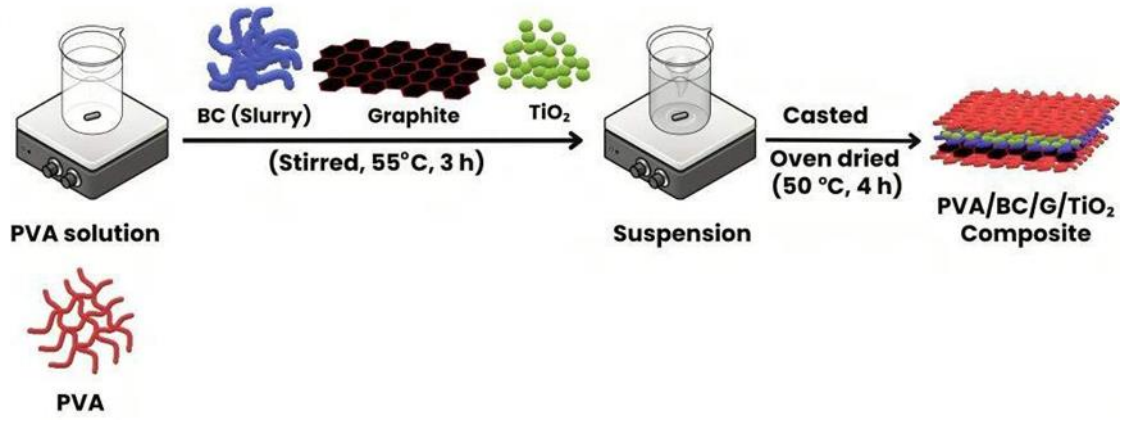

Figure 2. Schematic illustration of a method for synthesized PVA/BC/G/TiO_2 composite

Fabrication of PVA-Based Composite

According to Figure 2, the PVA-matrix composite was created using the casting method with some modifications to the procedure by Zhang et al.[14]. Solvated PVA was prepared by dissolving 5 g of PVA in a 50 mL methanol and water mixture (1:1) and stirring at 120°C for 1 hour. Then, a BC slurry of 10 g was sonicated for 30 minutes and added to the PVA solution. The mixture was stirred at 55°C for 1 hour, and graphite (0.375 g) was added, followed by titanium dioxide (0.7 g). The mixture was stirred again at 55°C for 1 hour. Finally, potassium persulfate 4% (w/v) was added to the suspension as an initiator agent for 30 minutes at 55°C. The resulting PVA/BC/G/TiO_2 suspension was molded and dried at 50°C for 4 hours.

Physical and Mechanical Tests

To calculate composite thickness, a digital screw micrometer (T&E CR1632) was used to measure the average thickness of 10 randomly selected spots from the sample, following—equation 1.

$$\bar{t} = \frac{t1 + t2 + \ldots + tn}{n} \quad (1)$$

The $\bar{t}$ indicates the average thickness, t is the thickness at a certain point, and n is the number of test points. The porosity test is carried out by immersing a sample cut in a circular shape in 80% n-butanol (v/v) and then calculating it based on equation 2.

$$\phi = \frac{(Mb - Mk)}{\rho B \times Vk} \times 100\% \quad (2)$$

Where, $Vk = \pi \times r^2 \times t$ (3)

DOI: https://doi.org/ 10.25077/jrk.v15i2.692

The sample was measured in terms of its dry mass (Mk) and wet mass (Mb), with ϱB indicating the density of n-butanol, Vk describing the dry volume of the sample, and r representing the sample's radius. The elongation of the composite at break (10 × 10 cm) was determined using an INSTRON 5567 with a 5.0 kN load cell to determine its tensile strength. The test according to ASTM D638 tensile strength[15]. The received data was then processed with the average formula equation 4, determining tensile strength and Young's Modulus.

$$\sigma_t = \frac{Ft}{At} \quad (4)$$

Ft is the tensile force perpendicular to the surface, and At is the sample area.

Swelling Behavior

The weight of the dry sample (M) and the sample after it was submerged (Mo) in a pH 6.86 buffer solution at room temperature were used to calculate the swelling behavior. Equation 5 was then used to determine the degree of swelling.

$$S = \frac{(Mo - M)}{M} \times 100\% \quad (5)$$

Kinetical Drug Release

The Arikibe et al. procedure was utilized to ascertain the TCH drug release kinetics[16]. After being soaked in a TCH solution, the composite sample was dried, and its maximum TCH wavelength was determined in a buffer solution with a pH of 6.86. A stock standard solution was prepared, diluted, and examined at a 200–400 nm wavelength using a UV-Vis spectrophotometer to generate a TCH standard curve. The drug release kinetics in a pH 6.86 medium were measured using the dissolution test method over 4 hours with 30-minute intervals. The data were fitted to first-order, zero-order, Higuchi, Hixon Crowell, and Kosmeyer-Peppas equations to choose the kinetic model[17].

Antibacterial Tests

The disc diffusion method was used to test the antibacterial activity of samples using Staphylococcus aureus bacteria obtained from FMIPA, Mataram University's Advanced Biological Laboratory. To assess the antibacterial activity of a 20 mm^2 composite, it was incubated at 37 °C for 24 hours in an agar medium in a petri dish. The inhibition zone was then measured[18].

Results and Discussion

Physical and Mechanical Properties

Porosity is a unit expressing the number and size of pores in composites. Porosity could be affected by the density of the composites; the more filler is successfully dispersed into the matrix, the more the density of the composite will increase[19][20]. Table 1 shows that composites have different thicknesses, due to the fabrication method, BC-matrix uses impregnation while the PVA-matrix uses casting. Also in Table 1, composites with BC-matrix have a higher porosity than PVA-matrix; adding filler can decrease porosity. This is also found in research by Al-Mihyawi & Al-Hussaini.[18], BC's porosity decreased by adding filler (alginate/Ag) at 7.98%. A similar thing was found in the PVA matrix; adding filler in Mohamed et al. decreased the porosity[21]. The research found that the porosity of PVA decreases with the addition of Al_2O_3 due to the trapping of filler in the pores between PVA molecular chains.

Furthermore, the mechanical ability was tested through a tensile strength test. According to Figure 3 and Table 1, BC has the highest tensile strength value and high porosity as well, due to its unique properties of BC, the structure of BC consists of microfibrils free of lignin and hemicellulose in the form of a 3D network structure caused it to be able to provide high pore geometry and mechanical strength at the same time[4]. Also according to Figure 3, the mechanical capability of composite with BC-matrix has decreased due to the uneven distribution of stress and pressure with the

addition of filler G and TiO_2[15][22]. Interaction between matrix with filler G reduced the mechanical ability of BC-matrix composites due to CTAB interaction with BC and PVA molecules; CTAB can reduce O-H bonds through its interaction with the matrix, as occurred in the study by Susilo et al.[23]; CTAB successfully reduces the mechanical ability of BC/G composites by 66,70%. Unlike the BC-matrix, composite with PVA-matrix has increased mechanical ability after adding fillers due to a more even fillers dispersion that causes the stress distribution to become more thorough[15][22].

FTIR Spectra

Composite characterization using FTIR instrumentation aims to determine and identify the presence of functional groups of composites. Typical absorption of pure BC synthesized using *G. xylinus* in coconut media based by Sarkono et al.[24] gives rise to the -OH stretching absorption peak at 3356,14 cm^{-1}. According to Figure 4, the absorption peak of -OH in BC was indicated by the appearance of a peak at 3344 cm^{-1}[8], this peak then shifted into a smaller wavenumber at 3332 cm^{-1}[11] in BC/G/PVA/TiO_2 composite; due to interaction between BC-matrix with filler[14]. The appearance of stronger -OH absorption peaks in composites with BC-matrix describes the higher number of hydrogen bonds still present in BC molecules[25].

Similarly, BC has a C-H stretching vibration peak observed at 2934 cm^{-1}, this is supported by the appearance of C-H bending at 1462 cm^{-1}. This peak shifts to a lower wavenumber due to the addition of fillers in both of BC-matrix and PVA-matrix[25].

Table 1. Data result of physical and mechanical properties

Sample	Thickness (mm)	Porosity (%)
BC	0.044	47.985
BC/G/PVA/TiO_2	0.101	41.698
PVA/BC/G/TiO_2	0.314	21.820

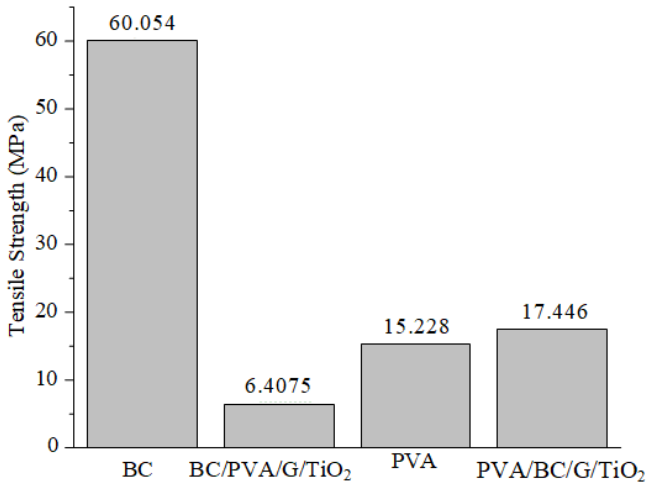

Figure 3. Tensile strength graph of composites

DOI: https://doi.org/ 10.25077/jrk.v15i2.692

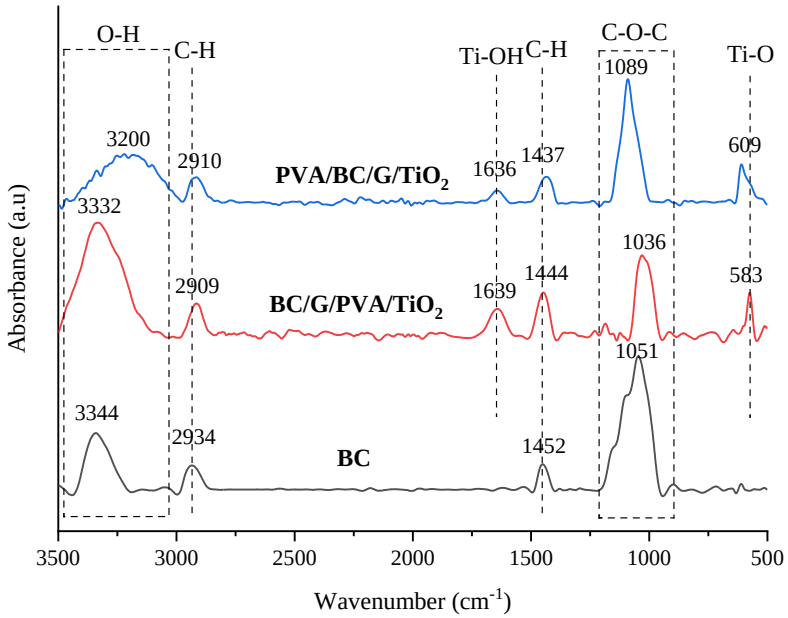

Figure 4. FTIR Spectra of BC/G/PVA/TiO_2 and PVA/BC/G/TiO_2

Besides that, absorption band -OH in the PVA-matrix composite was successfully detected at 3200 cm^{-1}[14]; this peak is shifted to a lower wavenumber than Vo et al.[26] research about absorption -OH band in pure PVA, detected at 3337,6 cm^{-1}. This means that there is an interaction between the PVA matrix and fillers. According to Figure 4, the C-O-C bond in the BC spectrum was suppressed in the BC/G/PVA/TiO_2 and PVA/BC/G/TiO_2 spectra due to the TiO_2 molecules attached to the surface of the two composites. Also, the appearance of Ti-OH stretching absorption bands at 1636 cm^{-1} and 1639 cm^{-1} indicates that TiO_2 molecules successfully enter both composite materials[25], supported by Ti-O bending absorption at 500-700 cm^{-1} in the fingerprint region[27].

Chemical Properties of Composite

The interaction between matrix and filler of composites is presented in Figure 5. According to Figure 5. graphite interacts with BC with the aid of CTAB as a surfactant. The hydrophobic tail of CTAB molecule will interact with graphite, while ammonium (N^+), as the hydrophilic head of CTAB, interacts with BC-matrix through electrostatic bonding[23]. Unlike BC-matrix, according to Figure 5. b, the composite with PVA-matrix successfully interacts with graphite with the aid of a potassium persulfate. Potassium persulfate is an initiator agent that promotes the oxidation process of PVA into PVA molecules that have vinyl acetate groups, which is hydrophobic[28],[29],[30]. Similar to the CTAB interaction, vinyl acetate groups interact with graphite through hydrophobic interactions, while the hydrophilic groups will interact with BC through H-bonding[31].

Next, the interaction of TiO_2 with both matrixes is presented in Figure 6. The TiO_2 metal distributed in composite BC and PVA-matrix surface interacted through H-bonding of atoms O on TiO_2 and atoms H in BC and PVA molecules[32].

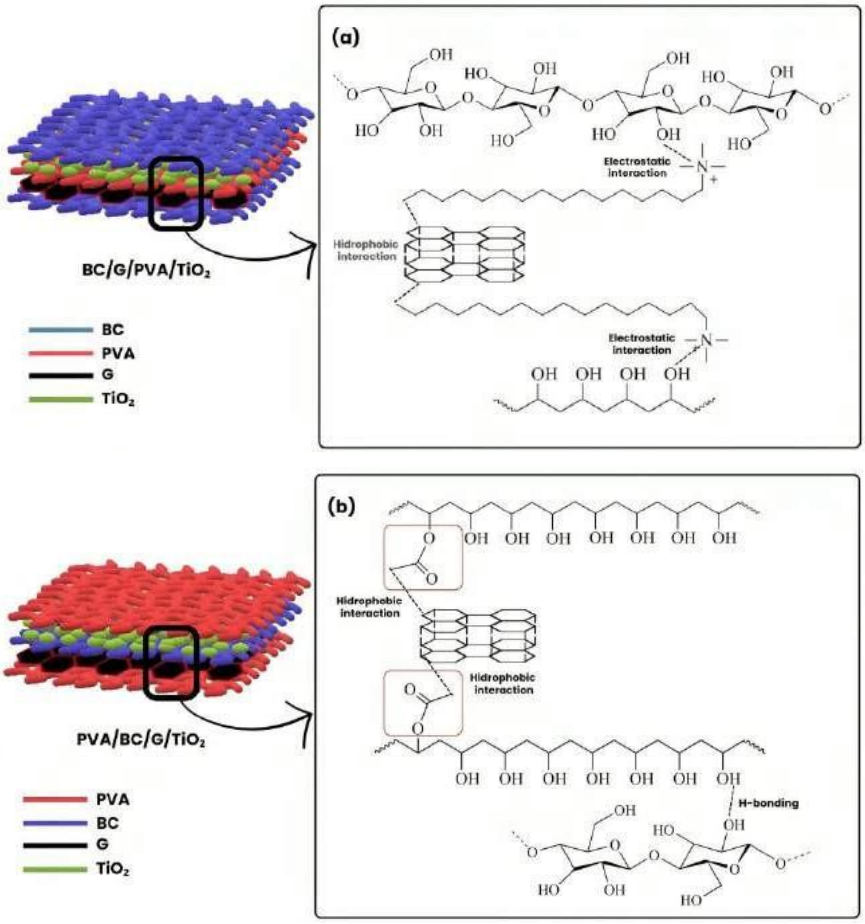

Figure 5. Illustration of interaction matrix BC (a) PVA (b) with filler in composites

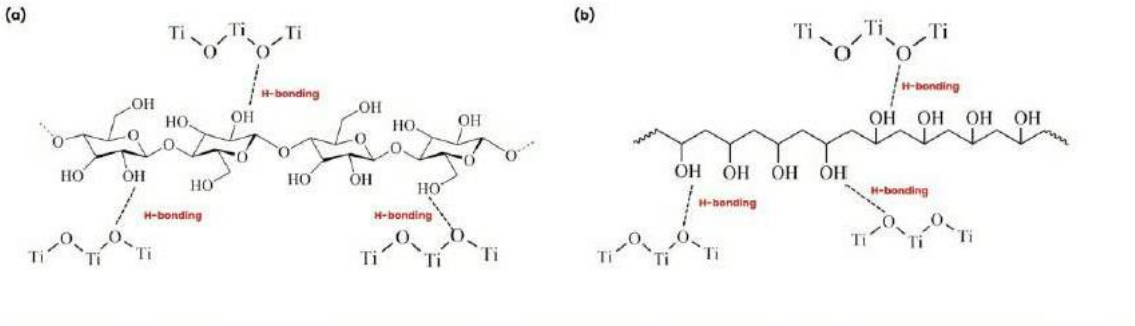

Figure 6. Illustration of interaction matrix BC (a) PVA (b) with TiO_2 in composites

Swelling Behavior

Studying the swelling behavior of composites to be applied in the medical field is very important, primarily to regulate the loading and release of drugs[16]. The swelling ratio of composites are affected by several things, like density, hydrophilicity, pH, temperature, and so forth[33].

DOI: https://doi.org/ 10.25077/jrk.v15i2.692

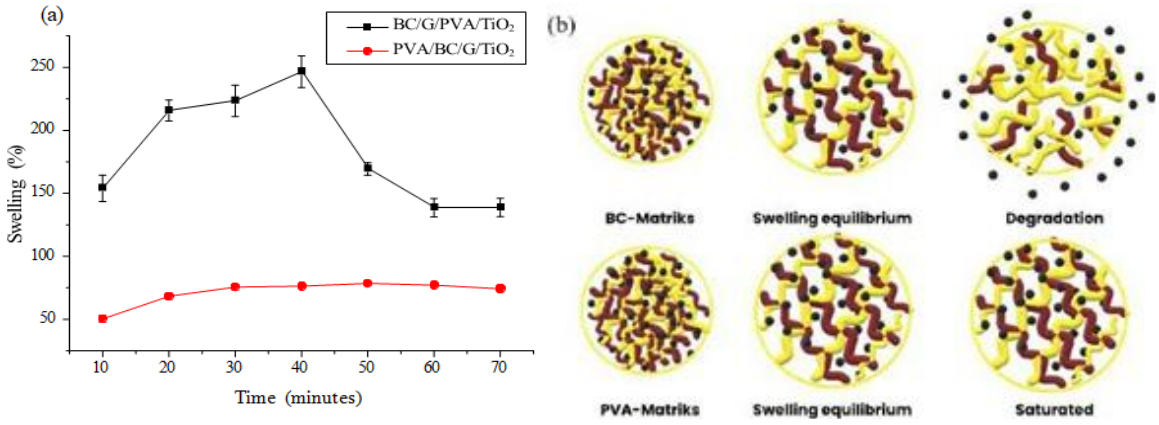

Figure 7. Graph of swelling behavior of BC and PVA-Matrix composites in time variations (a); Illustration of the swelling process in BC and PVA-Matrix composites (b)

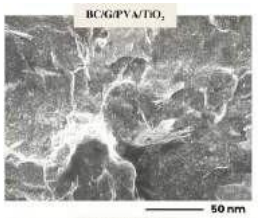

Element	Mass (%)	Atom (%)
C	12.94 ± 0,24	22.27 ± 0,42
O	45.11 ± 1.05	58.31 ± 1.36
S	3.66 ± 0.13	2.36 ± 0.08
K	5.41 ± 0.19	2.86 ± 0.10
Ti	32.88 ± 0.60	15.19 ± 0.26
Total	100.00	100.00

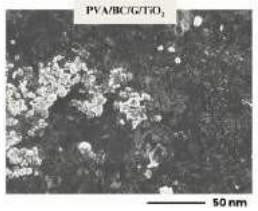

Element	Mass (%)	Atom (%)
C	18.19 ± 0,30	27.27 ± 0,46
O	54.66 ± 1.07	61.53 ± 1.20
S	3.72 ± 0.14	2.09 ± 0.08
K	3.49 ± 0.16	1.61 ± 0.07
Ti	19.94 ± 0.50	7.50 ± 0.19
Total	100.00	100.00

Figure 8. EDS result of BC/G/PVA/TiO_2 (a); PVA/BC/G/TiO_2 composite

According to Figure 7. a BC/G/PVA/TiO_2 composite has a more extraordinary swelling ability than PVA/BC/G/TiO_2. Composite with BC-matrix degrades after reaching swelling equilibrium (~40 minutes) due to the glycosidic breakdown in BC molecules by water contact[34]. Unlike BC-matrix, composites with PVA-matrix have a lower swelling ability and don't degrade due to filler interaction in composites. Figure 5. b shows that interaction between PVA-matrix and filler occurs through H- H-bonding and hydrophobic interactions. These hydrophobic interactions have more vital interaction compared to electrostatic interaction in BC-matrix, leading to a decreased chance of degradation due to the repulsion of water molecules, which is hydrophilic[35].

Morphological properties

The results of composite characterization prove the presence of all elements in composites using EDX instrumentation, demonstrating that all aspects detected in both composites are the same. Based on Figure 8, both composites give rise to the Ti element, which describes the presence of TiO_2 molecules[11]. Elements of potassium (K) and sulfur (S), with a small percentage, arise due.

The appearance of these elements is due to several things such as incomplete radical reactions of potassium persulfate ($K_2S_2O_8$) as an initiator. If incomplete radical reactions of potassium persulfate initiators ($K_2S_2O_8$) caused by optimal conditions aren't achieved within 1 hour (80 °C)[36], the preliminary neutralization process can also affect[37].

Drug Release Profile

According to Figure 9, the release of TCH drugs from both composites occurred in two stages with R^2 and k values shown in Table 2.

Based on Table 2, the kinetical drug release model of BC-matrix composite in the first stage is Zero Order with the highest R^2 value. This model describes that the release of the TCH from the composite isn't affected by differences in concentration, so it is suitable for application as a release medium for antibiotics and blood pressure guards that require constant release over time[38]. Next, PVA-matrix composites have a First-Order drug release kinetics model in the first stage (R=0,9981), like Sankarganesh et al.[15], the First Order model successfully describes the drug release kinetics of PVA-matrix composite, where the concentration in composite and release medium affects the drug release faster in the initial phase to reach equilibrium. Still, it impacts the slow release in the later phase because the rupture of the release phase has already been passed[39].

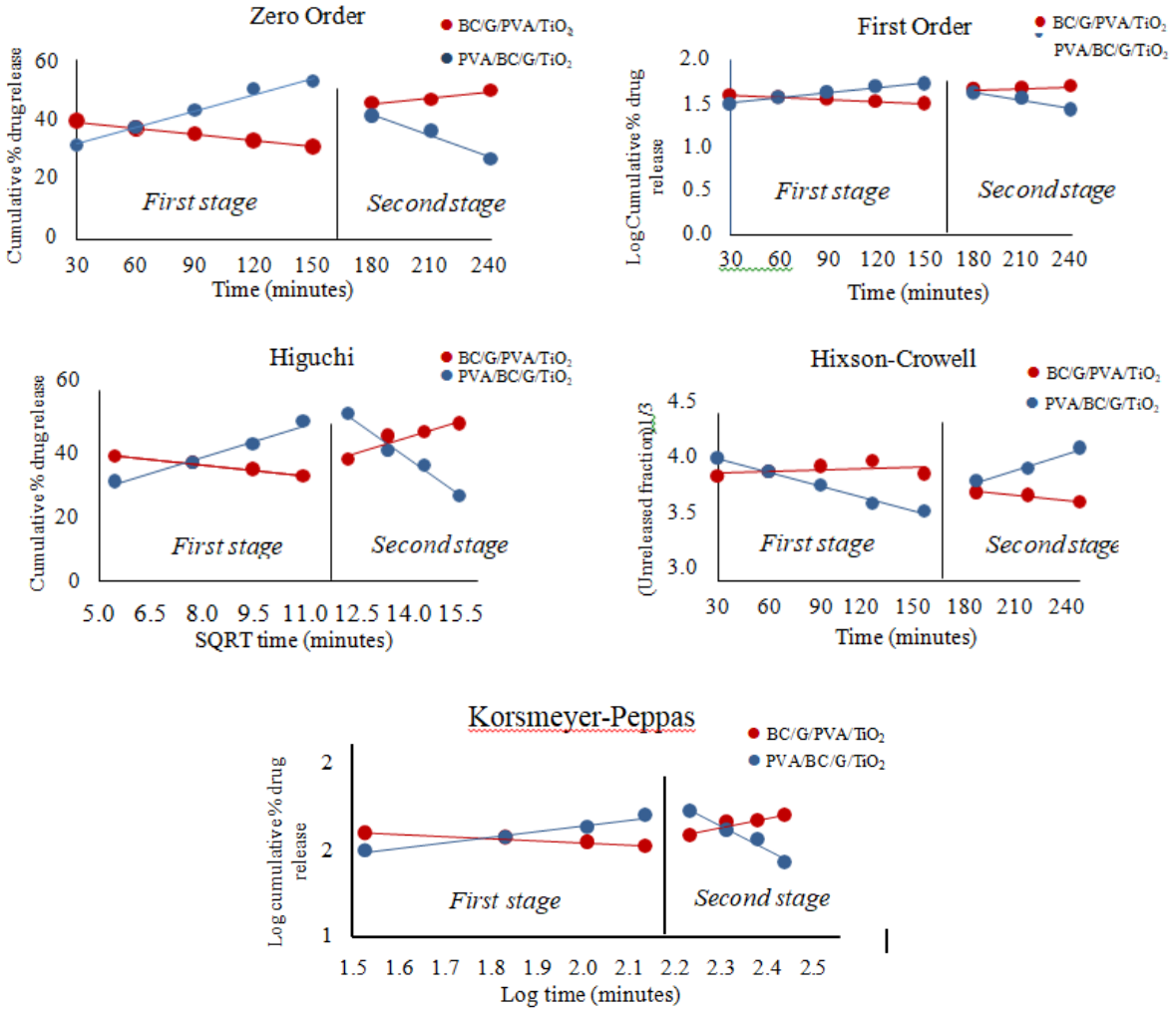

Figure 9. Kinetical drug release of BC/G/PVA/TiO_2 and PVA/BC/G/TiO_2 composites plotted as Zero Order, First Order, Higuchi, Hixson-Crowell, and Korsmeyer-Peppas model.

DOI: https://doi.org/ 10.25077/jrk.v15i2.692

Table 2. Kinetical modeling result of TCH drug release in two based composites

Model	Composites							
	BC matrix*		BC matrix**		PVA matrix*		PVA matrix**	
	R^2	k	R^2	k	R^2	K	R^2	k
Zero Order	1,0000	-0,0701	0,7760	0,1906	0,9974	0,2053	0,9795	-0,2761
First Order	0,9993	-0,0008	0,7460	0,0021	0,9981	0,0022	0,9795	-0,0031
Higuchi	0,9902	-1,1456	0,8991	3,2782	0,9805	3,3430	0,9827	-7,6708
Hixon-Crowell	0,9999	0,0015	0,8915	-0,0027	0.9936	-0,0045	0,9709	0,0060
Korsmeyer Peppas	0,9503	0,1223	0,8993	0,5237	0,9729	0,3266	0,9685	-1,3738

*First stages = 30-150 minutes; **Second stages = 150-240 minutes

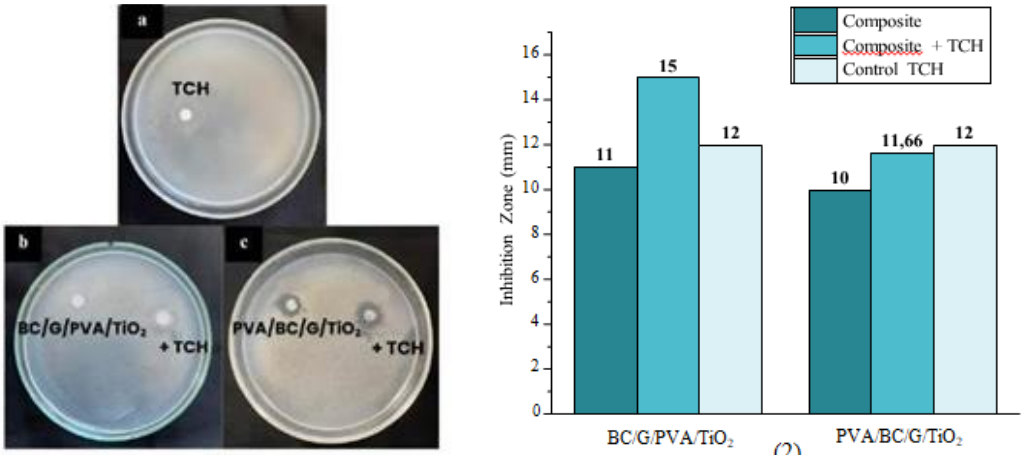

Figure 10. Antibacterial activity composite against *S. aureus* (1) Control (a); BC/G/PVA/TiO_2 (b); PVA/BC/G/TiO_2 (c); Graph of inhibition zone composite (2)

Antibacterial Activity

Tetracycline hydrochloride is an antibiotic that can inhibit microbial activity; this study used TCH as an additional antibacterial agent through diffusion[40]. The graph in Figure 10. (2) showed that both composites had antibacterial activity before and after the addition of TCH antibiotics. Due to fillers such as graphite and TiO2 already having antibacterial activity, graphite and TiO2 can inhibit bacterial activity by damaging bacterial cells by targeting bacterial cell walls. [12], [41].

Conclusions

Composites with BC and PVA matrices were successfully synthesized using different methods, namely impregnation and casting. The study process of drug release kinetics based on the kinetical model found that the TCH drug release in both composites with matrix variation is generally controlled by diffusion. TCH drug release kinetics in composite with BC-matrix followed Zero Order in the first stage and Kormeyer-Peppas in the second stage, while composite with PVA-matrix followed First Order in the first stage and Higuchi in the second stage. Adding TCH in both BC/G/PVA/TiO_2 and PVA/BC/G/TiO_2 composites increased antibacterial activity. The results show that both composites can be applied to promising biomedical fields.

Acknowledgments

We appreciate the access to the advanced chemistry laboratory at Mataram University, the integrated laboratory of Mataram State Islamic University, and the financial support

provided by the PNBP fund of Mataram University. These resources benefit testing, data collection, and result interpretation. These two universities' research environments have created a collaborative and inventive one that has enabled academic success.

References

1. Adepu, S. & Ramakrishna. S., Controlled Drug Delivery Systems: Current Status and Future Directions. *Molecules*., **26(19)**: 1-45 (2021). doi: 10.3390/molecules26195905.
2. Rouabhia, M., Asselin, J., Tazi, N., Messaddeq, Y., Levinson, D., & Zhang, Z., Production of Biocompatible and Antimicrobial Bacterial Cellulose Polymers Functionalized by RGDC Grafting Groups and Gentamicin. *ACS Appl Mater Interfaces*., **6(3)**: 1439–1446 (2014). doi: 10.1021/am4027983.
3. Alavarse, A. C., Silva. F. W. O., Colque, J. T., Silva, V. M., Prieto, T., Venancio, E. C., & Bonvent, J. J., Tetracycline Hydrochloride-Loaded Electrospun Nanofibers Mats Based on PVA And Chitosan For Wound Dressing. *Materials Science and Engineering C*., **77(1)**: 271–281(2017). doi: 10.1016/j.msec.2017.03.199.
4. Moniri, M., Moghaddam, A. B., Azizi, S., Rahim, R. A., Ariff, A. B., Saad, W. Z., Navaderi, M., & Mohamad, R., Production and Status of Bacterial Cellulose in Biomedical Engineering. *Nanomaterials*., **7(9)**: 1-26 (2017). doi: 10.3390/nano7090257.
5. Baker, M. I, Walsh, S. P., Schwartz, Z., & Boyan, B. D., A Review of Polyvinyl Alcohol and Its Uses in Cartilage and Orthopedic Applications. *Journal of Biomedical Materials Research - Part B Applied Biomaterials*., **100 B(5)**: 1451–1457 (2012). doi: 10.1002/jbm.b.32694.
6. Leitão, A. F., Silva, J. P., Dourado, F. & Gama, M., Production and Characterization of a New Bacterial Cellulose/Poly(Vinyl Alcohol) Nanocomposite. *Materials*., **6(5)**: 1956–1966 (2013), doi: 10.3390/ma6051956.
7. Busuioc, C., Isopencu, G. O., & Deleanu, I. M., Bacterial Cellulose–Polyvinyl Alcohol Based Complex Composites for Controlled Drug Release. *Applied Sciences (Switzerland).*, **13(2)**:1–13(2023).doi: 10.3390/app13021015.
8. Shao, W., Liu, H., Wang, S., Wu, J., Huang, M., Min, H., & Liu, X., Controlled Release and Antibacterial Activity of Tetracycline Hydrochloride-Loaded Bacterial Cellulose Composite Membranes. *Carbohydr Polym*., **145(1)**: 114–120 (2016). doi: 10.1016/j.carbpol.2016.02.065.
9. Manurung, R., Simanjuntak, S., Sembiring, J., Zaluku, E. C., Napitupulu, R. A. M., & Sihombing, S., Analisa Kekuatan Bahan Komposit Yang Diperkuat Serat Bambu Menggunakan Resin Polyester dengan Memvariasikan Susunan Serat Secara Acak dan Lurus Memanjang. *SjoME*., **2(1)**: 28-35 (2020). doi: 10.36655/sprocket.v2il.296
10. Aritonang, H. F., Wulandari, R., & Wuntu, A. D., Synthesis and Characterization of Bacterial Cellulose/Nano-Graphite Nanocomposite Membranes. *Macromol Symp*., **391(1)**: 1–7 (2020). doi: 10.1002/masy.201900145.
11. Sharma, D., Kumari, M., & Dhayal, V., Fabrication and Characterization of Cellulose/PVA/TiO_2 Nanocomposite Thin Film as a Photocatalyst. *Materials Today: Proceedings.*, **43(1)**: 2970–2974 (2021). doi: 10.1016/j.matpr.2021.01.323.
12. Liauw, C. M., Vaidya, M., Slate, A. J., Hickey, N. A., Ryder, S., Periñán, E. M., McBain, A. J., Banks, C. E., Whitehead, A., Analysis of Cellular Damage Resulting from Exposure of Bacteria to Graphene Oxide and Hybrids Using Fourier Transform Infrared Spectroscopy. *Antibiotics*., **12(4)**: 1-20 (2023). doi: 10.3390/antibiotics12040776.
13. Pathakoti, K., Manubolu, M., & Hwang, H.-M., Effect of Size and Crystalline Phase of TiO_2 Nanoparticles on Photocatalytic Inactivation of Escherichia coli. *J Nanosci Nanotechnol*., **19(12)**: 8172–8179 (2019). doi: 10.1166/jnn.2019.16757.
14. Zhang, L., Zheng, S., Zhong, L., Wang, Y., Zhang, X., & Xue, J., Preparation of Polyvinyl Alcohol/Bacterial-Cellulose-

 DOI: https://doi.org/ 10.25077/jrk.v15i2.692

Coated Biochar-Nanosilver Antibacterial Composite Membranes. *Applied Sciences (Switzerland)*., **10(3)**: 1-13 (2020). doi: 10.3390/app10030752.

15. Maulana, J., Suryanto, H., & Aminnudin, Y., Effect of Graphene Addition on Bacterial Cellulose-Based Nanocomposite. *Journal of Mechanical Engineering Science and Technology (JMEST)*., **6(2)**: 107-118 (2022). doi: 10.17977/um016v6i22022p107.
16. Arikibe, J. E., Lata, R., & Rohindra, D., Bacterial Cellulose/Chitosan Hydrogels Synthesized In situ for Biomedical Application. *Journal of Applied Biosciences*., **162(1)**: 16675–16693 (2021). doi: 10.35759/jabs.162.1.
17. Sankarganesh, P., Parthasarathy, V., Kumar, A. G., Ragu, S., Saraniya, M., Udayakumari, N., & Anbarasan, R., Preparation of Cellulose-PVA Blended Hydrogels for Wound Healing Applications With Controlled Release of the Antibacterial Drug: an In Vitro Anticancer Activity. *Biomass Convers Biorefin*., **1(1)**: 1-12 (2022). doi: 10.1007/s13399-022-02586-y.
18. Al-Mihyawi, R., & Al-Hussaini, N. A., Preparation and Characterization of Bacterial Cellulose/Natural Polymer Antibacterial Composites. *International Journal of Research in Agricultural Sciences*., **4(1)**: 2348-3997 (2017).
19. Xu, K., Qin, Y., Xu, T., Xie, X., Deng, J., Qi, J., & Huang, C., Combining Polymeric Membranes with Inorganic Woven Fabric: Towards the Continuous and Affordable Fabrication of a Multifunctional Separator for Lithium-Ion Battery. *Journal of Membrane Science.*, **592(1)**: 1-9 (2019). doi: 10.1016/j.memsci.2019.117364.
20. Nuryati, R. Amalia, R., & Hairiyah, N., Pembuatan Komposit dari Limbah Plastik Polyethylene Terephthalate (PET) Berbasis Serat Alam Daun Pandan Laut (*Pandanus tectorius*). *Jurnal Agroindustri*., **10(2)**: 107-118 (2020). doi: 10.31186/j.agroind.10.2.107-117.
21. Mohamed, H. F. M., Hady, E. E. A., Moneim, M. M. Y., Bakr, M. A. M., Soliman, M. A. M., Shehata, M. G. H., & Ismail, M. A. T., Effect of Al_2O_3 on Nanostructure and Ion Transport Properties of PVA/PEG/SSA Polymer Electrolyte Membrane. *Polymers*., **14(19)**: 1-18 (2022). doi: 10.3390/polym14194029.
22. Shirkavad, S., & Moslehifard, E., Effect of TiO_2 Nanoparticles on Tensile Strength of Dental Acrylic Resins. *J Dent Res Dent Clin Dent Prospects*., **8(4)**: 197–203 (2014). doi: 10.5681/joddd.2014.036.
23. Susilo, B. D., Suryanto, H., & Aminnudin, A., Characterization of Bacterial Nanocellulose - Graphite Nanoplatelets Composite Films. *Journal of Mechanical Engineering Science and Technology*., **5(2)**: p. 145-154 (2021). doi: 10.17977/um016v5i22021p145.
24. Sarkono, S. Moeljopawiro, B. Setiaji, and L. Sembiring., Physicochemical Properties of Cellulose Produced by Bacterial Isolate Gluconacetobacter xylinus KRE-65 in Different Fermentation Methods," *AGRITECH*., **35(4)**: 434–440 (2015). doi: 10.22146/agritech.9327.
25. Khalid, A., Ullah, H., Ul-Islam, M., Khan, R., Khan, S., Ahmad, F., Khan, T., & Wahid, F., Bacterial Cellulose-TiO_2 Nanocomposites Promote Healing and Tissue Regeneration in Burn Mice Model. *RSC Adv*., **7(75)**: 47662–47668 (2017). doi: 10.1039/c7ra06699f.
26. Vo, T. V., Dang, T. H., & Chen, B. H., Synthesis of Intelligent pH Indicative Films from Chitosan/Poly(Vinyl Alcohol)/Anthocyanin Extracted from Red Cabbage. *Polymers (Basel)*., **11(7)**: 1–12 (2019). doi: 10.3390/polym11071088.
27. Karim, S., Pardoyo, & Subagiyo, A., Sintesis dan Karakterisasi TiO_2 Terdoping Nitrogen (N-Doped TiO_2) dengan Metode Sol-Gel. *Jurnal Kimia Sains dan Aplikasi*., **19(2)**: 63–67 (2016). doi: 10.14710/jksa.19.2.63-67.
28. Li, F., Ma, H., Shen, C., Pan. Y., Zhang, Y., Liu, Y., Xu, C., & Wu, D., From the Accelerated Production of •OH Radicals to the Crosslinking of Polyvinyl Alcohol: The Role of Free Radicals Initiated by Persulfates. *Appl Catal B*., **258(1)**: 1-12 (2021). doi: 10.1016/j.apcatb.2020.119763.

29. Wang, S., Xie, K., & Tang, D., Benign Oxidation of PVA for Configuration of Reversible Polyketal Networks. *Eur Polym J.*, **140(1)**: 1-8 (2020). doi: 10.1016/j.eurpolymj.2020.110050.
30. Liu, J., Zhang, Y., Li, H., Liu, C., Quan, P., & Fang, L., The Role of Hydrophilic/Hydrophobic Group Ratio of Polyvinyl Alcohol on The Miscibility of Amlodipine in Orodispersible Films: From Molecular Mechanism Study to Product Attributes. *Int J Pharm.*, **630** (2023). doi: 10.1016/j.ijpharm.2022.122383.
31. Masood, S., Gulnar, L. D., Arshad, H., Rehman, W., & Atique, A., Preparation and Optical Characterization of Poly (Vinyl Alcohol) and Starch (Native And Modified) Blend Films. *Journal of Polymer Research.*, **29(12)**: 1-17 (2022). doi: 10.1007/s10965-022-03332-8.
32. Abodif, A. M., Meng, L., Sanjrani, M., Ahmed, A. S. A., Belvett, N., Wei, Z. Z., & Ning. D., Mechanisms and Models of Adsorption: TiO_2-Supported Biochar for Removal of 3,4-Dimethylaniline. *ACS Omega.*, **5(23)**: 13630–13640 (2020). doi: 10.1021/acsomega.0c00619.
33. Păvăloiu, R.D., Stoica-Guzun, A., & Dobre, T., Swelling Studies of Composite Hydrogels Based On Bacterial Cellulose and Gelatin. *U P B Sci.Bull Series B.*, **77(1)** 2015.
34. Basu, P., Saha, N., Alexandrova, R., & Saha, P., Calcium Phosphate Incorporated Bacterial Cellulose-Polyvinylpyrrolidone Based Hydrogel Scaffold: Structural Property and Cell Viability Study for Bone Regeneration Application. *Polymers.*, **11(11)**: 1-24 (2019). doi: 10.3390/polym11111821.
35. Xiao, F., Chen, Z., Wei, Z., & Tian, L., Hydrophobic Interaction: A Promising Driving Force for the Biomedical Applications of Nucleic Acids. *Advanced Science.*, **7(6)**: 1-34 (2020). doi: 10.1002/advs.202001048.
36. Ortiz, D. G., Nouxet, M., Maréchal, W., Lorain, O., Deratani, A., & Pochat-Bohatier, C., Immobilization of Poly(Vinyl Pyrrolidone) in Polysulfone Membranes by Radically-Initiated Crosslinking Using Potassium Persulfate. *Membranes (Basel).*, **12(7)**: 1-17 (2022). doi: 10.3390/membranes12070664.
37. Czarnecka E., & Nowaczyk, J., Semi-Natural Superabsorbents Based on Starch-G-Poly(Acrylic Acid): Modification, Synthesis and Application. *Polymers (Basel).*, **12(8)**: 1-19 (2020). doi: 10.3390/polym12081794.
38. Khattab M. M., & Dahman, Y., Functionalized Bacterial Cellulose Nanowhiskers as Long-Lasting Drug Nanocarrier for Antibiotics and Anticancer Drugs. *Canadian Journal of Chemical Engineering*., **97(10)**: 2594–2607 (2019). doi: 10.1002/cjce.23566.
39. Paarakh, M., Jose, P., Setty, C., & Christoper, G., Release Kinetics-Concepts and Applications. *International Journal of Pharmaceutical Research & Technology.*, **10(1)**: 12–21 (2018). doi: 10.31838/ijprt/08.01.02.
40. Liyaskina, E. V., Revin, V. V., Paramonova, E. N., Revina, N. V., & Kolesnikova, S. G., Bacterial Cellulose/Alginate Nanocomposite for Antimicrobial Wound Dressing. *KnE Energy*., **3(2)**: 202-211(2018). doi: 10.18502/ken.v3i2.1814.
41. Malmir, S., Karbalaei, A., Pourmadadi, M., Hamedi, J., Yazdian, F., & Navaee, M., Antibacterial Properties of a Bacterial Cellulose CQD-TiO_2 Nanocomposite. *Carbohydr Polym*., **234(1)**: 1-10 (2020). doi: 10.1016/j.carbpol.2020.115835.